Kyushu University Global COE Program
Journal of Novel Carbon Resource Sciences, Vol. 7, pp. 1-6, Feb. 2013

Biomechanical Effect of Implantation of Chitosan/MWNTs Reinforced Scaffold into Damaged Femur

Sunghyen Hwang[*1], Mistugu Todo[*2]

[*1]Interdisciplinary Graduate School of Engineering Sciences, Kyushu University
[*2]Research Institute for Applied Mechanics, Kyushu University

(Received October 29, 2012; accepted November 29, 2012)

Scaffold is one of the important factors in the regenerative medicine which could allow tissues growth and support structure during the repair. However, most of the synthetic polymer based scaffolds have not enough mechanical properties for bone regeneration. Recently, reinforced scaffolds have been proposed to solve these problems. When the scaffolds are implanted in the human body, it is important to predict the effect after implantation. In this study, biomechanical effects of reinforced scaffolds with different types of reinforcement materials implanted into a damaged femur were analyzed using the CT-image based finite element analysis. It was found that the scaffold with Chitosan/MWNTs reinforcement is very effective to achieve a biomechanical compatibility with natural bone tissue.

1. Introduction

Femur is one of the primary parts for supporting the body and the longest and strongest bone in the body. It allows different kinds of movement for human life such as walking, jogging, and sitting. Femoral fractures sometime occur by accidents and/or doing exercise with aging. Yoshimura et al., has reported 120,000 cases of femoral fracture annually in Japan[1)]. The most common types of femoral fractures are transverse fracture, oblique fracture, spiral fracture, comminuted fracture, and open fracture. Recently, femoral fracture in young people has been reported. These fractures are frequently due to high-energy collision. The most common cause is car or motorcycle accident. This tendency has increased rapidly[2)]. In other words, most of patients with femoral damage are caused by normal activity in their lives[3-4)]. Standard fractures of femur can be simply cured by the normal fixation of the damaged part, however, when a fracture is recognized as a crush type, then implantation of autograft, allograft or artificial bone substitutes need to be considered.

Recently, tissue engineering approach has widely been considered as an advanced surgical treatment. In the bone tissue engineering approach, porous materials called scaffold are used to regenerate bone tissue with use of stem cells. Synthetic biodegradable polymers, natural polymers, bioactive ceramics and their composites have been used to construct the porous scaffolds[5-6)]. It is however noted that most of those materials lack mechanical properties for bone regeneration. To solve this problem, composite and/or reinforced structures have been suggested by some researchers. They used synthetic polymer based reinforced structures, calcium-based bio-ceramics and biocompatible chitosan/MWNTs scaffolds[7-9)]. These scaffolds with reinforced materials exhibited good mechanical properties with proper porosity and biocompatibility. Among them, bio-ceramic composite scaffolds and chitosan/MWNTs scaffolds have similar mechanical properties of bone tissue. Especially, chitosan/MWNTs scaffolds have the best mechanical properties for bone regeneration. Effects of scaffold implantation to femur have been investigated by several researchers[10-12)]. It is however still difficult to understand such effects precisely, mainly because of the complex structure of femur consisting of thick cortical and porous cancellous bones[13-15)].

Finite element (FE) analysis of scaffold for bone tissue engineering has been performed by several researchers[16-21)]. Detailed porous microstructures of scaffolds have been investigated by considering their mechanical properties and using micro-CT images[16,17)]. Scaffolds implanted into bone models have also been analyzed by FE models to investigate the biomechanical compatibility[18-21)]. For example, a tibial model was developed using CT-images and porous polymeric scaffold was implanted just beneath the condylar surface[18,19)]. Kelly constructed a simplified joint model with scaffold to investigate tissue regeneration within the scaffold[20)]. A rabit bone model was developed using CT-images and a scaffold was implanted into the bone to optimize the structural properties of the scaffold[21)]. However, these computational approaches did not consider the stress distribution within the bone models and the most of scaffold had single porous structures with single materials.

The purpose of this study was to characterize the effects of reinforced scaffolds having different kinds of reinforcement materials on the mechanical condition of a femur. A FE model of the femur was developed from CT images of a patient. Stress analysis by the FE method was then performed to compare the stress fields in the vicinity of the scaffolds to determine better biomechanical compatibility.

2. Methods

The contralateral femur of a 45 years male patient

(weight: 60 kg) was used in the analysis. In order to construct a 3D finite element model, the geometry of the femur was obtained by CT data. Fig. 1. shows the created FE model and the boundary conditions. It was assumed that the femoral model can be constructed as a two-phase model consisting of cortical and cancellous parts. Damage regions (may be caused by fracture or remove of tumor) in the FE model were assumed to exist in the femoral shaft. The location of implanted scaffold is shown in Fig. 2. Three different FE models were constructed by changing the ratio of the damage area to the original cross-sectional area (6264 mm^2) of the femoral shaft: (A) damage area 30% (1879 mm^2), (B) 50% (3132 mm^2) and (C) 70% (4534 mm^2) as shown in Figs. 2 and 3. Scaffolds were then implanted into the damage regions so that the size of the scaffold was perfectly fit to that of the damage part. These scaffolds have a two-phase structure, the outer shell as reinforcement and the inner porous core. The details of the implanted scaffolds are shown in Fig. 4. The inner core was assumed to be made from a biodegradable polymer PCL, and the shell reinforcement was made from biodegradable polymer PLLA, polymer/bioceramic composite PLLA/HA, or chitosan/MWNTs. The weight fractions of these composites are also shown in Fig.4. The thickness of the scaffolds, i.e. the damage regions, was 30 mm and the thickness of the reinforcement shell was 5 mm.

Young's modulus and Poisson's ratio of cancellous and cortical bone were determined from the references[22-25]. In these references, Young's modulus of cortical bone has been reported in a range from 4 to 30 GPa[22,23] and Young's modulus of cancellous bone to be from 250 to 730 MPa[24,25]. In the present work, Young's moduli of cortical and cancellous bones were simply determined by taking the average values of all the data found in the references. The material properties of the shell reinforcement and the porous core of the scaffold were determined from experiment and literature. PLLA pellets (TOYOTA Co.), PCL pellets (Daicel Chemistry Industries Co.) and HAp particles (Sangi Co., Ltd.) were used to fabricate scaffolds. The average molecular weights of PLLA and PCL were $M_w = 2.2 \times 10^5$ and 1.4×10^5 g/mol, respectively. The phase separation and freeze-drying methods were used to fabricate the scaffolds. The detail of fabrication procedure can be found in our previous work[7]. Young's modulus of chitosan/MWNT was found in the reference[9].

These values of Young's modulus and the Poisson's ratio are summarized with the element types in Table 1.

The boundary conditions shown in Fig.1 were normally accepted by researchers[16]. A vertical load of 1800N, which was calculated as the three times of the weight (60 kg × 3 with gravity), was applied at the bottom of the femoral shaft. The femoral head was fixed in all direction and rotations, as a first approximation of the condition of natural hip joint. The number of elements of the normal model without scaffold was 95,800 and the numbers of elements of Type A, B and C models were 100,618, 100,659 and 100,652, respectively. The stress analyses of these models were then performed by a commercial finite element code.

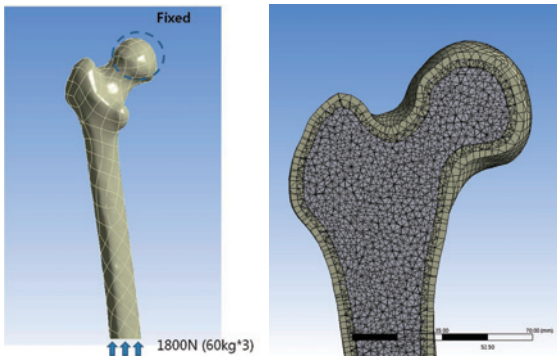

Fig. 1 Three-dimensional femur model and boundary conditions for FEA.

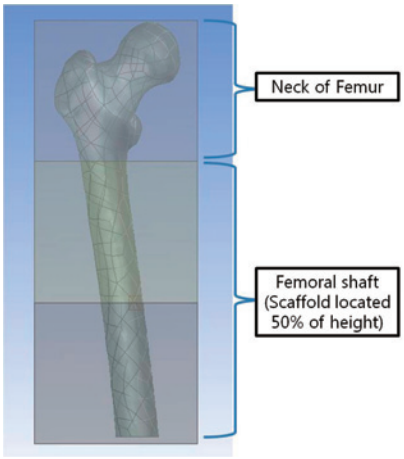

(a) Location of scaffold implantation

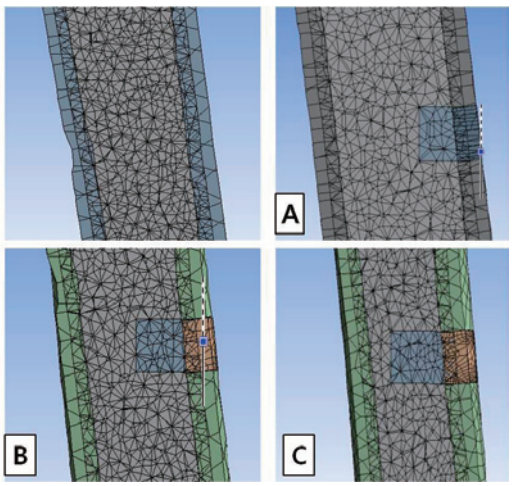

(b) Femoral shaft models with scaffolds

Fig. 2 Femur model with implanted scaffold.

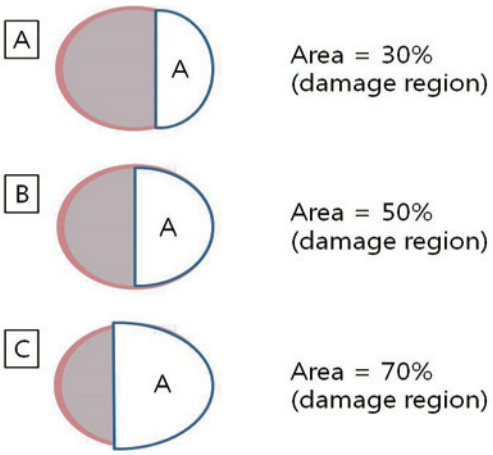

Fig. 3 Three different damage regions.

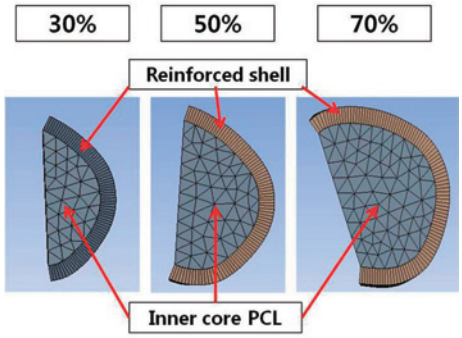

Inner core	Reinforced shell
PCL 7wt%	PLLA (100wt%) PLLA/HA (90wt% : 10wt%) Chitosan/MWNTs (98wt% : 2wt%)

Fig. 4 Details of damage regions and scaffolds.

Table 1 Element type and material properties

Material	Young's modulus	Poisson's ratio	Elements type
PCL	1.40 MPa	0.4	Solid, Porous
PLLA	300 MPa	0.4	Shell
PLLA/HA	400 MPa	0.4	Shell
Chitosan/MWNTs	2.15 GPa	0.3	Shell
Cortical bone	17 GPa	0.3	Solid
Cancellous bone	484 MPa	0.3	Solid

3. Results and discussion

Distributions of von-Mises stress in the normal and the type A models are shown in Fig. 5. The normal model showed that a distribution of high stress concentration was dispersed from the neck to the shaft of femur with maximum stress in the cortical bone of 17.6 MPa. The PLLA and PLLA/HA models exhibited the high stresses were mainly concentrated at the edges of the scaffolds. The maximum stress values in the PLLA and PLLA/HA models were 53.6 and 49.5 MPa, respectively, and much higher than that of the normal model. On the contrary, the distribution pattern of stress in the chitosan/MWNTs model was quite similar to that in the normal model, and the maximum stress was 25.7 MPa which was much lower than those in the PLLA and PLLA/HA models. The von-Mises stress distributions in the type B and C models are shown in Figs. 6 and 7, respectively.

In the PLLA and PLLA/HA models, the stresses were again severely concentrated at the edge of the scaffolds within the femoral shafts. The maximum stress values were 79.7 MPa in the PLLA model and 67.9 MPa in the PLLA/HA model which were much higher than that of the normal model (17.6 MPa). On the other hand, in the chitosan/MWNTs model, the stress concentration region was distributed from the neck to the shaft of the femur, although the high stress concentration also existed at the edge of the scaffold. The maximum stress was 29.7 MPa which was much lower than those of the PLLA and PLLA/HA models. The distribution patterns of stress concentration in the type C models were very similar to those in the type B models, although the maximum stress values were much higher (157.8 MPa in the PLLA, 108.6 MPa in the PLLA/HA and 35.0 MPa in the chitosan/MWNTs).

These results clearly show that the larger damage area caused higher stress concentration. However, the average rate of increase of the maximum stress to increase of the damage area was very different and the chitosan/MWNTs model showed the lowest rate. Actually, such rate of the chitosan/MWNTs model was 4.09 kPa/mm^2, while the rates of the PLLA and the PLLA/HA models were 64.8 and 58.0 kPa/mm^2, respectively.

The maximum values of equivalent, shear and principal stresses are shown in Fig. 8. In all the models, the stresses in the normal model were the lowest, and chitosan/MWNTs model exhibited the lowest stress levels of all the three scaffold models. The Young's modulus of chitosan/MWNTs (2.15 GPa) lies between the cancellous bone (484 MPa) and the cortical bone (17 GPa), while the moduli of PLLA and PLLA/HA (300 and 400 MPa) are much lower than those of bones. It is thus considered that the chitosan/MWNTs reinforcement shell plays a role of cortical bone at the damage region. This clearly indicates that the chitosan/MWNTs reinforced scaffold has much better biomechanical compatibility than the PLLA and PLLA/HA scaffolds, and may enhance bone regeneration within the damage region. It should be

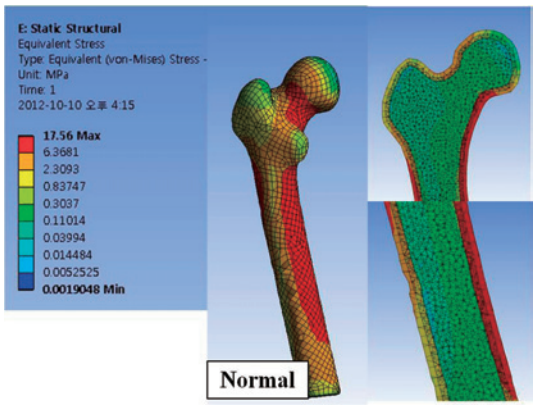

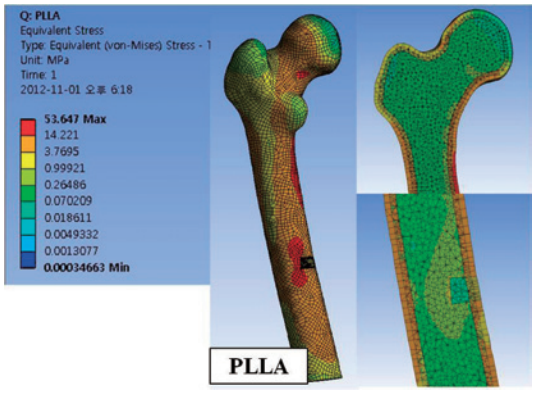

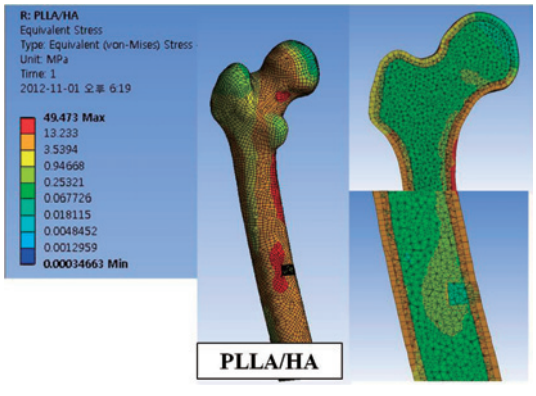

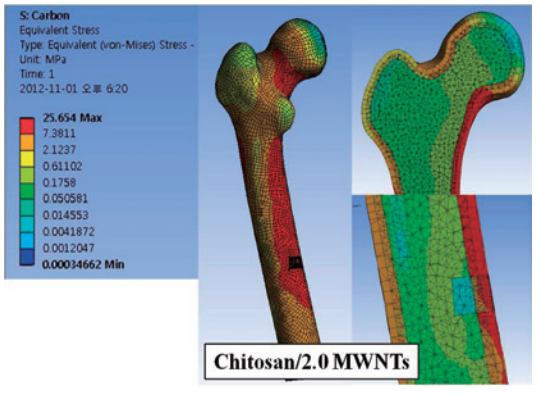

Fig. 5 Distribution of von-Mises stress in the normal and Type A models.

however noted that bioactive ceramics such as calcium phosphates (HA and β-TCP) are known to activate bone regeneration, and therefore PLLA/HA reinforced scaffold may also have good biocompatibility, although its biomechanical compatibility is lower than the chitosan/MWNTs reinforced scaffold. It is noted that the modulus of chitosan/MWNTs may be able to increase by increase the weight fraction of MWNTs within the composite material to improve the biomechanical compatibility. It was however reported that the change of modulus was very small when the fraction of MWNTs was increased[9]. Further study is needed to clarify such effect of MWNTs content on the modulus of nano composite materials.

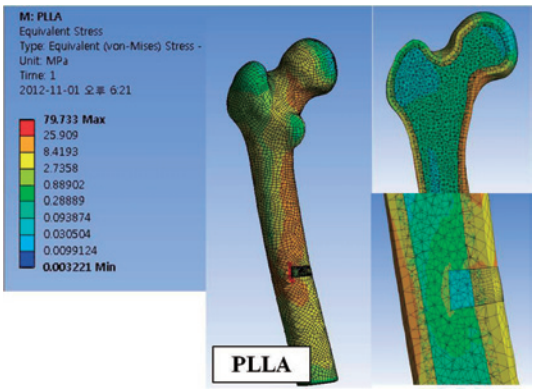

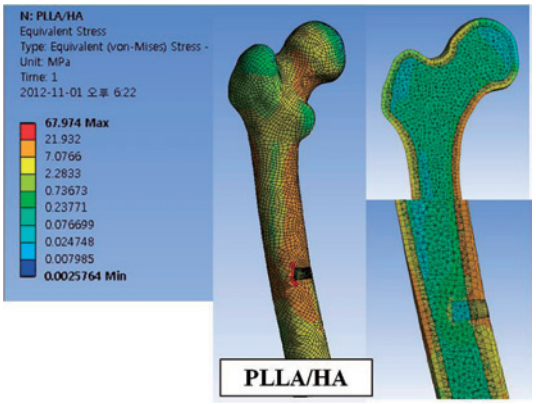

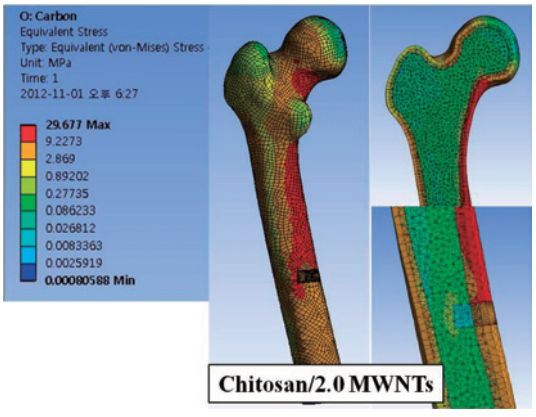

Fig. 6 Distribution of von-Mises stress in the normal and Type B models.

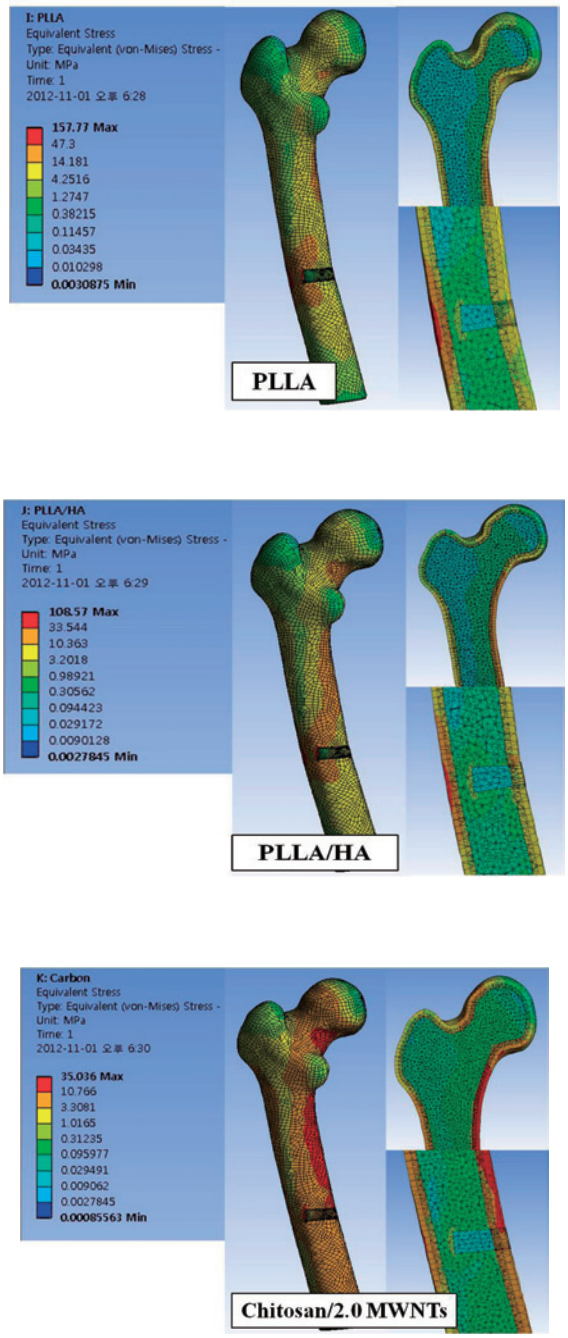

Fig. 7 Distribution of von-Mises stress in the normal and Type C models.

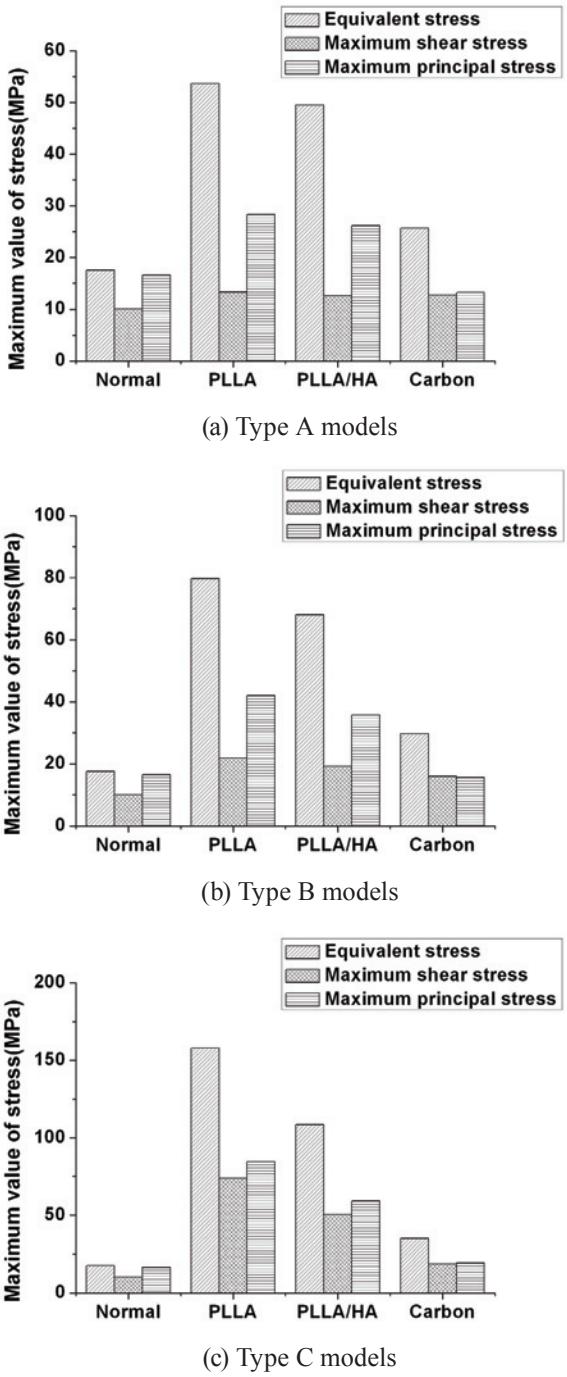

(a) Type A models

(b) Type B models

(c) Type C models

Fig. 8 Comparison of maximum equivalent, shear and principal stress values.

4. Conclusion

A finite element model of a femur was developed from the CT images of a patient. A cylindrical reinforced scaffold consisting of porous core and reinforced shell was implanted into a damage region of the femoral shaft by assuming three different areas. It is also presumed that the core was made from PCL, and the shell was made from PLLA, PLLA/HA or chitosan/2.0% MWNTs. A vertical load was applied to the bottom of the femoral model with the femoral head restricted completely, and stress analysis was performed.

The results of the analysis clearly showed that the distribution profile of the von-Mises stress in the chitosan/MWNTs model was similar to that in the normal model without scaffold because the Young's modulus of chitosan/MWNTs is close to that of the cortical bone. On the other hand, in the PLLA and PLLA/HA models, the stress was severely concentrated at the edge of the

scaffolds as a result of large difference of the Young's modulus between PLLA (or PLLA/HA) and the cortical bone. It is thus concluded that the chitosan/MWNTs reinforced scaffold may have the best biomechanical compatibility for bone regeneration in the damaged femur.

References

1) N. Yoshimura, T Suzuki, T. Hosoi, and H. Orimo, *J. Bone Miner Metabo.*, **23**(1), 78 (2005).
2) A. J. Starr, M. T. Hay, C. M. Reinert, D. S. Borer, and K. C. Christensen, *J. Orthop. Trauma*, **20**(4), 240 (2006).
3) R. Hedlund, and U. Lindgren, *J. Orthop. Res.*, **5**(2), 242 (1987).
4) R. C. Steven, M. B. Dennis, C. N. Michael, S. B. Warren, A. C. Jane, K. G. Harry, R. M. Stephen, C. S. Jean, G. S. Dana, S. Peter, and M. V. Thomas, *J. Ameri. Medi. Assoc.*, **263**(5), 665 (1990).
5) C. Damien and R. Parsons, *J. Appl. Biomat.*, **2**, 187 (1991).
6) R. Langer and J. P. Vacanti, *J. Orthop. Res.*, **9**, 641 (1993).
7) J. E. Park and M. Todo, *J. Mater. Sci. : Mater. Med.*, **22**(5), 1171 (2011).
8) D. W. Hutmacher, J. T. Schantz, C. X. F. Lam, K. Cl Tan, T. C. Lim, *J. Tissue Eng. Regen. Med.*, **1**(4), 245 (2007).
9) S. F. Wang, L. S. Zhang, W. D. Zhang, and Y. J. Tong, *Biomacromolecules*, **6**, 3067 (2005).
10) B. Rai, M. E. Oest, K. M. Dupont, K. H. Ho, S. H. Teoh, and R. E. Guldberg, *J. Biomed. Mater. Res.*, **81A**(4), 888 (2007).
11) M. E. Oest, K. M. Dupont, H. J. Kong, D. J. Mooney, and R. E. Guldberg, *J. Orthop. Res.*, **25**(7),941 (2007).
12) L. Meinel, O. Betz, R. Fajardo, S. Hofmann, A. Nazarian, E. Cory, M. Hilbe, J. McCool, R. Langer, G. Vunjak - Novakovic, H. P. Merkle, B. Rechenberg, D. L. Kaplan, C. Kirker-Head, *Bone*, **39**(4), 922 (2006).
13) J. D. Currey, *J. Biomech.*, **21**(2), 131 (1988).
14) J. C. Rice, S. C. Cowin, J. A. Bowman, *J. Biomech.*, **21**(2), 155 (1988).
15) J. Seebeck, J. Goldhahn, H. Städele, P. Messmer, M. M. Morlock, E. Schneider, *J. Orthop. Res.*, **22**(6), 1237 (2004).
16) T. Van Cleynenbreugel, J. Schrooten, H. Van Oosterwyck, and J. Vander Sloten, *Med. Bio. Eng. Comput.*, **44**, 517 (2006).
17) D. Lacroix, A. Chateau, M.-P. Ginebra, and J. A. Planell, *Biomaterials*, **27**, 5326 (2006).
18) T. Van Cleynenbreugel, H. Van Oosterwyck, J. Vander Sloten, and J. Schrooten, *J. Mater. Sci.: Mater. Med.*, **13**, 1245 (2002).
19) S. V. N. Jaecques, H. Van Oosterwyck, L. Muraru, T. Van Cleynenbreugel, E. De Smet, M. Wevers, I. Naert, and J. Vander Sloten, *Biomaterials*, **25**, 1683 (2004).
20) D. J. Kelly and P. J. Prendergast, *Tissue Eng.*, **12**, 2509 (2006).
21) J. A. Sanz-Herrera, J. M. Garacia-Aznar, and M. Doblare, *Acta Biomaterialia*, **5**, 219 (2009).
22) J. E. M. Koivumaki, J. Thevenot, P. Pulkkinen, V. Kuhn, T. M. Link, F. Eckstein, and T. Jamsa, *Bone*, **50**, 824 (2012).
23) J. H. Keyak, S. A. Rossi, K. A. Jones, H. B. Skinner, *J. Biomech.*, **31**(2), 125 (1997).
24) T. S. Keller, *J. Biomech.*, **27**, 1159 (1994).
25) B. A. Varghese, M. E. Miller, and T. N. Hangartner, *J. Musculoskelet Neurnal Interact*, **4**(8), 379 (2008).